Observation of Supershell Structure in Alkali Metal Nanowires

A.I. Yanson[1], I.K. Yanson[1,2], and J.M. van Ruitenbeek[1]
[1] *Kamerlingh Onnes Laboratorium, Universiteit Leiden, Postbus 9504, NL-2300 RA Leiden, The Netherlands*
[2] *B. Verkin Institute for Low Temperature Physics and Engineering, National Academy of Sciences, 310164, Kharkiv, Ukraine*

Nanowires are formed by indenting and subsequently retracting two pieces of sodium metal. Their cross-section gradually reduces upon retraction and the diameters can be obtained from the conductance. In previous work we have demonstrated that when one constructs a histogram of diameters from large numbers of indentation-retraction cycles, such histograms show a periodic pattern of stable nanowire diameters due to shell structure in the conductance modes. Here, we report the observation of a modulation of this periodic pattern, in agreement with predictions of a *supershell* structure.

Metallic nanowires clearly exhibit quantum properties in their conductance and structure. At the level of a few atoms in cross-section the conductance through metallic nanowires can be described in terms of a finite number of quantum modes, and it has been shown that this number is determined by the number of valence orbitals of the metal atoms involved [1–3]. For monovalent free-electron metals such as gold and, in particular, the alkali metals the conductance in the smallest contacts evolves roughly through the successive opening of distinct conductance channels as the contact size increases [4–6]. This quantum character of electrical transport was already inferred from histograms of conductance values for atomic-size point contacts, which show that the contacts have a preference for multiples of the conductance quantum $G_0 = 2e^2/h$ [7,8], after correction for a small series resistance.

It had been suggested that the formation of quantum modes in nanowires should not only determine the conductance but also the cohesive energy [9–11]. Recently, we have shown that the stability of nanowires in the range of cross-sections up to about 130 atoms is determined by electronic shell structure for quantum modes [12]. The shell structure was observed in conductance histograms, which were measured by many times indenting and retracting two metal electrodes by means of a mechanically controllable break junction (MCBJ) [13]. The key evidence for shell structure is a regular spacing of diameters for wires with enhanced stability, where the diameters were obtained from the semiclassical expression for the conductance [14]. The shell structure observed here is a close analogue of the shell structure observed for alkali metal clusters [15,16], and it is the same principle that also applies to electrons in atoms and to protons and neutrons in nuclei.

For metal clusters produced in vapor jets in vacuum, and analyzed by mass selection, it was observed that clusters with certain 'magic numbers' of atoms, 8, 20 ,40 , 58, etc., are more abundant than others. This was explained by their enhanced stability due to the closing of the shells of electronic states, modeled as free electron waves confined to a spherical potential well. The magic numbers can even be obtained from a semiclassical expansion for the oscillating part of the density of single-particle levels [15,17,18], where the stable clusters are determined by those diameters for which a bouncing electron wave traveling along a closed classical path inscribed inside the spherical cluster walls obeys the Bohr-Sommerfeld quantization condition with the bulk metal Fermi wave vector, k_F. The possible trajectories are illustrated in Fig. 1. It was shown that for spherical clusters the triangular and square orbits, with indices $(3,1)$ and $(4,1)$, dominantly determine the magic number series.

Since the two dominant orbits, triangle and square, lead to slightly different series of stable diameters, the interference between the two series gives rise to a beat pattern, known as *super*shell structure [15,17,19]. For alkali metal clusters a single beat due to this effect has indeed been reported [20,21]. Here, we report the observation of supershell structure in sodium nanowires. We show that, in contrast to clusters but in agreement with the theory for nanowires, the diametric orbit (labeled $(2,1)$ in Fig. 1) has a strong contribution. Due to the larger

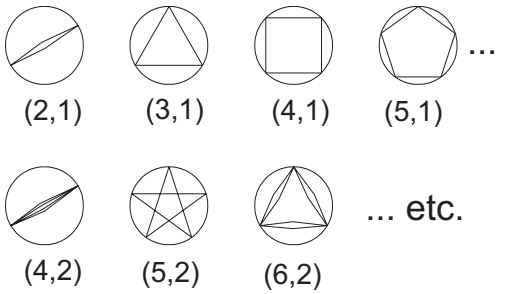

FIG. 1. Series of semiclassical orbits inscribed inside a circular cross-section, which are applicable to spheres (clusters) and cylinders (nanowires) alike. The orbits are labeled as (M,Q), where M is the number of vertices and Q is the winding number

separation between the periods for diametric and higher orbits, several beat minima of the supershell structure can be observed.

The experiment is performed using an MCBJ, modified to accommodate the very reactive alkali metals [8]. A rectangular piece of sodium metal is cut, while immersed in paraffin oil for protection against oxidation, and fixed upon a phosphor bronze bending beam with four 1 mm screws. A notch is cut in the center of the sodium sample, and the assembly is taken out of the paraffin and quickly mounted in a sample holder in a three-point bending configuration. Current and voltage leads are connected to both sides of the notch and the sample holder is evacuated and cooled down to liquid helium temperature. By applying force to the bending beam the sodium sample is broken at the notch, by which two clean fracture surfaces are exposed. Atomic-size contacts can then be established by relaxing the force, using a piezoelectric element for fine control. A heater and thermometer permit controlling the temperature from 4.2 K to above 100 K, while the vacuum can remains immersed in liquid helium. The conductance of the contacts is measured with a four-point dc-voltage bias circuit. The signal goes via a current-to-voltage converter through a 16 bit, 10^5 samples/s analog-to-digital converter to a pc-based controller. The software also drives the two halves of the sample into and out of contact by controlling the piezovoltage. Conductance values are automatically accumulated into histograms for typically over 10^4 contact breaking cycles, with a resolution of about 10 bins per G_0. In order to reduce digitization noise a three bin wide smoothing function is applied to the histograms.

At low temperatures and low voltage bias only four pronounced peaks at low conductance are seen in the histogram, near 1, 3, 5 and 6 G_0, which have been attributed to the successive occupation of distinct quantum modes [8]. At higher conductance the histogram shows a number of rather wide hills which grow into sharp peaks as we increase the temperature [12]. Fig. 2a shows an example of a histogram for sodium at a sample temperature of 90 K. The histogram is similar to the one presented in Ref. [12], but the modulation of the peak intensities is more pronounced here [22]. The radius R of the nanowires can be obtained from the semiclassical expression for the conductance [14],

$$\frac{G}{G_0} = \left(\frac{k_F R}{2}\right)^2 \left(1 - \frac{2}{k_F R}\right). \qquad (1)$$

The inset in Fig. 2a shows the radii, in units k_F^{-1}, corresponding to the first 6 maxima against their sequential number. Indeed, for shell structure we expect regularly spaced peaks as a function of the radius.

The modulation of the peak intensities and their periodicity is more clearly illustrated by subtracting a smooth background and plotting the histogram as a function of the radius, see Fig. 2b. Two beat minima are clearly visible at about $k_F R \simeq 7$ and 11.5, and a third can be seen on the expanded scale in the inset. Similar modulations have been observed in histograms for potassium and lithium, which will be discussed elsewhere.

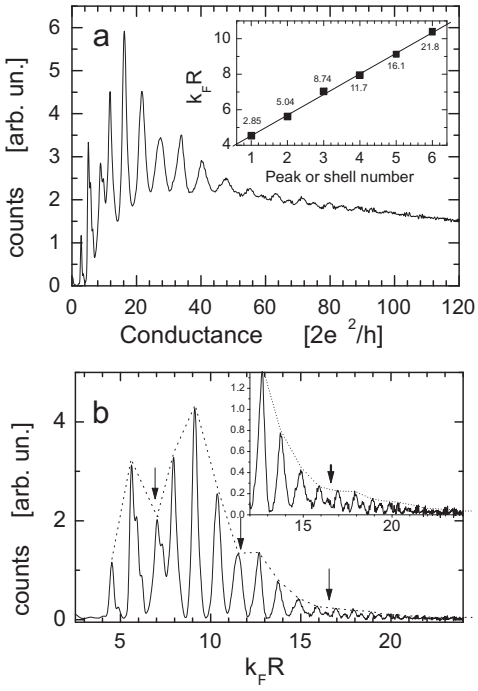

FIG. 2. Histogram of the number of times each conductance is observed. (a) Data taken for sodium at $T = 90$ K and bias voltage 100 mV, constructed from over 13800 individual indentation cycles. The inset shows a plot of the radii of the first 6 maxima versus the peak number, illustrating the regular spacing of the peak positions (the numbers represent conductance values for each peak in quantum units). (b) The conductance histogram for sodium from (a) with a smooth background subtracted, plotted against the radius. In the inset a magnified portion at high conductances is displayed. The dotted curve envelops peaks in the histogram and the arrows point to positions of minimal amplitude. These are the nodes of the supershell structure.

The components in the periodic structure are separated by making a Fourier transform of the curve in Fig. 2b, which is shown in Fig. 3a. We observe two frequency components, one at 0.6–0.65 and the other at 0.8–0.9 $(k_F R)^{-1}$. We will argue that these are the components of the supershell structure.

The quantum modes in a nanowire give rise to an oscillating contribution in the density of electronic states as a function of electron energy at constant radius or as a function of the radius of the wire at the Fermi energy. The modes each form a one-dimensional band, with quantum numbers determined by the confinement in the two transverse dimensions. This leads to an oscillating struc-

ture in the thermodynamic potential [9–11,23–25]. The latter determines the stability of a particular structure, which leads to an oscillating probability for nanowire diameters. Also the Sharvin conductance of the nanowires is modified by an oscillating contribution, but this contribution appears to be of secondary importance to the experiment [12]. The leading terms in a semiclassical expansion of the oscillating part of thermodynamic potential are [23],

$$\Omega^{osc} = \frac{2\varepsilon_F k_F}{\sqrt{2\pi r''r}} \sum_{M=2}^{\infty} \sum_{Q=1}^{M/2} \frac{1}{M^{7/2}} \left[\sin\left(\frac{\pi Q}{M}\right)\right]^{-3/2} \times \cos\left[2Mr\sin\left(\frac{\pi Q}{M}\right) + \frac{\pi}{2}\left(M+\frac{1}{2}\right)\right], \quad (2)$$

where $r = k_F R$, $r'' = \partial^2 r/\partial z^2$ is the curvature along the direction of the wire axis, and r and r'' are taken at the narrowest cross-section, $z = 0$. The number M corresponds to the number of vertices in the semiclassical orbit (see Fig 1) and Q is the winding number. In order to evaluate this expression we need to make some assumption about a smooth evolution of the curvature of the wire, but this will only affect the prefactor and not the oscillating structure itself. Following Ref. [23] we assume a parabolic wire shape, $r = r_0 + 4(A - r_o)(z/L)^2$. This shape grows smoothly from an initial cylindrical wire of length L_0 and radius A while maintaining a constant volume, so that the radius at the narrowest point can be expressed in terms of its length L as $r_0 = (A/4)(\sqrt{30L_0/L - 5} - 1)$. Substituting these expressions into Eq. 2 we calculate the Fourier transform of $\Omega^{osc}(r)$ in the same range of r as for the experimental data. The result is given in Fig. 3b, where we have included terms up to $M = 7$ for $Q = 1$ (the higher Q give rise to lower amplitude harmonics and we concentrate on the fundamental components). The dominant peak is due to the diametric orbit $(M, Q) = (2, 1)$ and the peaks for higher M rapidly decrease in amplitude and their frequency converges at 1, marking the end of the first series ($Q = 1$). In the Fourier transform we can only resolve two peaks in addition to the one for $M = 2$, corresponding to the triangular ($M = 3$) and square orbits ($M = 4$).

The experiment clearly shows the same groups of frequencies, one corresponding to the diametric orbit and one peak at the position of the triangular and square orbits, which cannot be individually resolved. Some of the higher frequency maxima with small intensities are probably partly due to harmonics of the main bands. The relative intensities of three calculated peaks cannot be directly compared to the theoretical spectrum since the latter results from the thermodynamic potential, which we do not measure directly. The experimental spectrum is derived from the conductance histogram and is expected to reflect the same components as the thermodynamic potential, but the intensities depend, amongst others, on kinetic factors for surface diffusion of atoms and the time available for reaching the proper minima in the potential. Further differences may arise from deviations in cylindrical symmetry of the wire and scattering of the electrons on residual surface roughness. In particular the later mechanism would favor the higher order orbits, since specular reflection increases for smaller angle of incidence with the surface.

In contrast to cylindrical systems, for spherical systems the diametric orbit ($M = 2$) is negligible as it has a significantly smaller degeneracy compared to the triangular ($M = 3$) and squared ($M = 4$) ones [17]: For a given position of one vertex the triangle and square have an additional degree of freedom being the rotation around the normal to this point. The contribution of the higher order orbits decays as a high power of the index M of the orbit. The closeness of the frequencies for the triangular and square orbits leads to a long beating period. The first node of the shell structure amplitude should be observed after approximately 12 periods of principal oscillations. The natural limit on the number of chemical elements makes the number of shells in the periodic table too small for supershell structure to be observable.

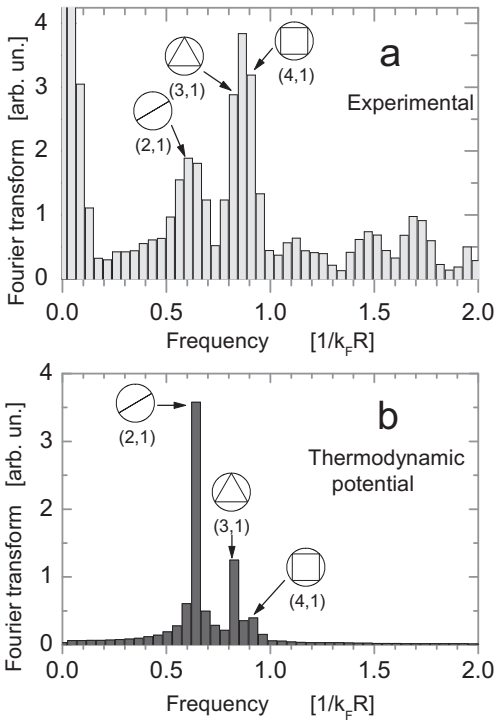

FIG. 3. (a) Fourier transform of the histogram of Fig. 2b for sodium. Two main peaks at 0.6–0.65 and 0.8–0.9 demonstrate the importance of the distinct contribution of the diametric orbit. (b) Fourier transform of the calculated oscillatory part of the thermodynamic potential, Eq. 2, including terms $Q = 1$ and $M = 2, 3, \ldots, 7$. The shape of the nanowire was set by the parameters $k_F L_0 = 200$ and $k_F A = 50$. The range of the variable r is chosen to be approximately the same as for the experimental histograms. The three main orbits, diametric, triangle and square, are indicated.

The same applies to shell structure in atomic nuclei. Although the amplitude of such a high number of oscillations is greatly diminished, the first node of the beating pattern in cluster abundance spectra was observed in Refs. [20,21,26].

For nanowires, the degeneracy of the diametric, triangle and square orbits is of the same order and the larger separation between the $M = 2$ frequency and the higher ones make the beating pattern more readily visible in the nanowire shell structure as compared to the metal cluster experiments. Thus, for the first time a direct Fourier transform of the experimental data yields proof for the existence of semiclassical orbits responsible for the oscillations in the thermodynamic potential of the system as a function of the radius.

[1] E. Scheer, P. Joyez, D. Esteve, C. Urbina, and M.H. Devoret, Phys. Rev. Lett. **78**, 3535 (1997).

[2] E. Scheer, N. Agraït, J.C. Cuevas, A. Levy Yeyati, B. Ludoph, A. Martín-Rodero, G. Rubio Bollinger, J.M. van Ruitenbeek, and C. Urbina, Nature **394**, 154 (1998).

[3] J.C. Cuevas, A. Levy Yeyati, and A. Martín-Rodero, Phys. Rev. Lett. **80**, 1066 (1998).

[4] H. van den Brom and J.M. van Ruitenbeek, Phys. Rev. Lett. **82**, 1526 (1999).

[5] B. Ludoph, M.H. Devoret, D. Esteve, C. Urbina, and J.M. van Ruitenbeek, Phys. Rev. Lett. **82**, 1530 (1999).

[6] B. Ludoph and J.M. van Ruitenbeek, Phys. Rev. B **61**, 2273 (2000).

[7] M. Brandbyge, J. Schiøtz, M. Sørensen, P. Stoltze, K.W. Jacobsen, J. Nørskov, L. Olesen, E. Lægsgaard, I. Stensgaard, and F. Besenbacher, Phys. Rev. B **52**, 8499 (1995).

[8] J.M. Krans, J.M. van Ruitenbeek, V.V. Fisun, I.K. Yanson, and L.J. de Jongh, Nature **375**, 767 (1995).

[9] C.A. Stafford, D. Baeriswyl, and J. Bürki, Phys. Rev. Lett. **79**, 2863 (1997).

[10] J.M. van Ruitenbeek, M.H. Devoret, D. Esteve, and C. Urbina, Phys. Rev. B **56**, 12566 (1997).

[11] C. Yannouleas and U. Landman, J. Phys. Chem. B **101**, 5780 (1997).

[12] A.I. Yanson, I.K. Yanson, and J.M. van Ruitenbeek, Nature **400**, 144 (1999).

[13] C.J. Muller, J.M. van Ruitenbeek, and L.J. de Jongh, Phys. Rev. Lett. **69**, 140 (1992).

[14] J.A. Torres, J.I. Pascual, and J.J. Sáenz, Phys. Rev. B **49**, 16581 (1994).

[15] M. Brack, Rev. Mod. Phys. **65**, 677 (1993).

[16] W.A. de Heer, Rev. Mod. Phys. **65**, 611 (1993).

[17] R. Balian and C. Bloch, Ann. Phys. (NY) **69**, 76 (1972).

[18] M. Brack and R.K. Bhaduri, *Semiclassical Physics*, (Addison-Wesley, Reading, Mass. 1997); S. Bjornholm and J. Pedersen, Nucl. Phys. News vol. 1, No. 6 (1991).

[19] H. Nishioka, K. Hansen and B.R. Mottelson, Phys. Rev. B **42**, 9377 (1990).

[20] J. Pedersen *et al.*, Nature **353**, 733 (1991).

[21] C. Bréchignac, Ph. Cahuze, F. Carlier, M. de Frutos and J.Ph. Roux, Phys. Rev. B **47**, 2271 (1993).

[22] The details of the histograms are a.o. influenced by the sample temperature and the bias voltage. Also, we expect that the crystal structure of the banks at either side of the nanowire will be of importance. We have no possibility to control this orientation, but it may be responsible for the slight variation in appearance of the histograms. The beat minima are not always equally pronounced, but their positions have been reproduced for several samples, and the two main frequency components can always be recognized in the Fourier spectrum.

[23] C. Yannouleas, E.N. Bogachek and U. Landman, Phys. Rev. B **57**, 4872 (1998).

[24] C. Höppler and W. Zwerger, Phys. Rev. B **59**, R7849 (1999).

[25] F. Kassubek, C.A. Stafford and H. Grabert, Phys. Rev. **59**, 7560 (1999).

[26] M. Pellarin, B. Baguenard, C. Bordas, J. Lermé and J.L. Vialle, Phys. Rev B **48**, 17645 (1993).